A PHOTOELECTRIC-PHOTOGRAPHIC STUDY OF THE NORMAL ALBEDO OF THE MOON

CONTRIBUTIONS TO ASTROGEOLOGY

Prepared on behalf of the National Aeronautics and Space Administration

GEOLOGICAL SURVEY PROFESSIONAL PAPER 599-E

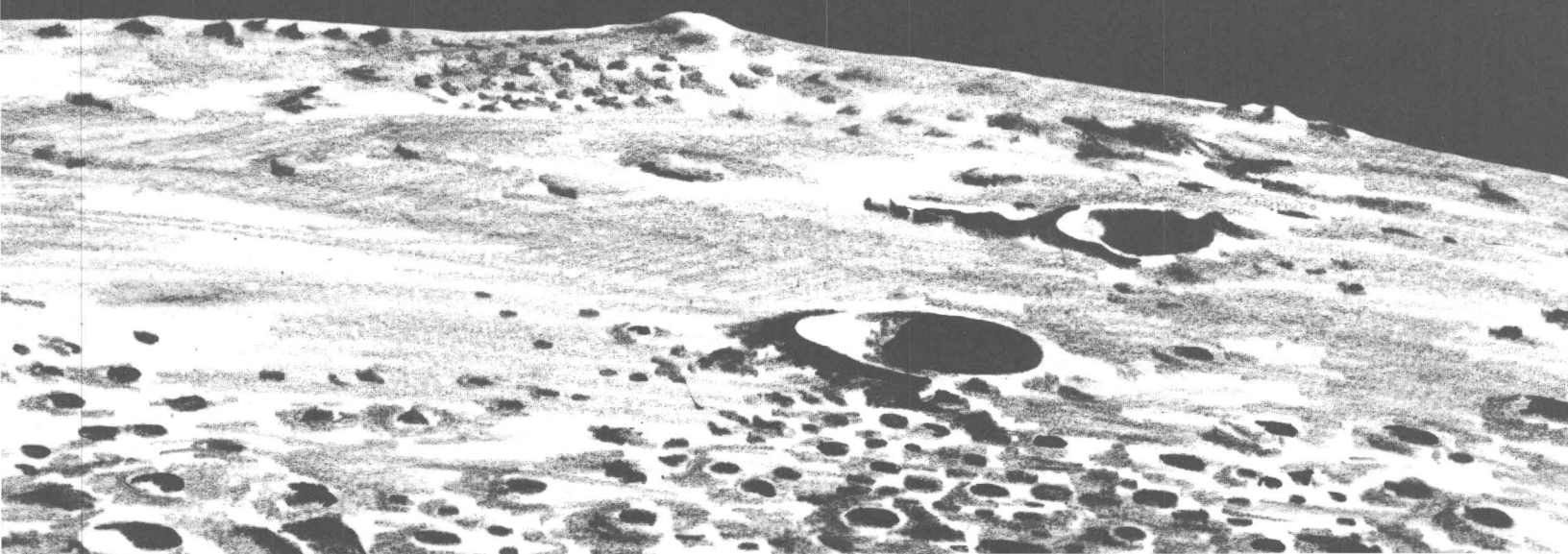

A Photoelectric-Photographic Study of the Normal Albedo of the Moon

By HOWARD A. POHN *and* ROBERT L. WILDEY

Accompanied by an ALBEDO MAP OF THE MOON

By HOWARD A. POHN, ROBERT L. WILDEY, *and* GAIL E. SUTTON

CONTRIBUTIONS TO ASTROGEOLOGY

GEOLOGICAL SURVEY PROFESSIONAL PAPER 599-E

Prepared on behalf of the National Aeronautics and Space Administration

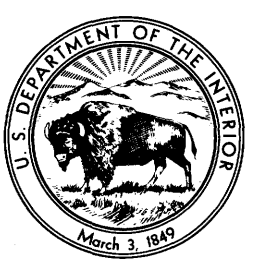

UNITED STATES GOVERNMENT PRINTING OFFICE, WASHINGTON : 1970

A PHOTOELECTRIC-PHOTOGRAPHIC STUDY OF THE NORMAL ALBEDO OF THE MOON

By HOWARD A. POHN and ROBERT L. WILDEY

ABSTRACT

A map of the normal albedo of the moon has been prepared by automatically measuring and raster-recording the optical density of a photoelectrically calibrated full-moon photographic plate. Calibration permits direct transfer of normal albedo (after reduction from the photoelectric signal recorded by the photometer) to the isodensity contours of the photographic image. On the night that the photographic and photoelectric observations were made, the lunar phase angle was 1.5°. Photoelectric observations of 182 points scattered across the lunar surface were correlated with the density of corresponding points on the photographic plate. Plate exposure coincided in time with the photoelectric photometry. The photographic emulsion-filter combination used provided a poorer approximation of the spectral bandpass of the Johnson photoelectric *V* magnitude than the emulsion-filter combination normally used for stellar photographic *V;* however, the spectroscopic emulsion used for stars is unnecessarily grainy and too fast for a photometric exposure. The moon's color is much more uniform than that of a field of stars; hence, the errors due to color effects that were introduced during calibration are insignificant. The photographic plate was transcribed as a density map at a scale of 1:5,000,000, using a Joyce-Loebl–Beckman-Whitley combination densitometer and code tracer. Steps were taken to reduce random error by insuring uniformity of the photographic process. This random error was measured to be about 1 percent. The range of normal albedo was divided into 20 contour intervals, with extremes of 7 and 23 percent at the 3″ of arc resolution employed. Reliability of the map is assured because, for the first time, simultaneous photoelectric calibration was utilized and the plate parameters were demonstrably uniform. The map has already proven to be of great utility in the fields of lunar geologic mapping and astronautical engineering.

INTRODUCTION

The primary principles of superposition, intersection, and topographic expression are fundamental to both terrestrial and lunar geologic mapping. Rock color, a secondary property useful on earth, cannot be used in mapping the moon because of the moon's lack of color diversity. The lunar surface does, however, exhibit a wide range of reflected surface brightness. Precise measurement of this brightness variation and its delineation are the subjects of this study.

Differences in reflected brightness of the lunar surface are obvious to the naked eye. Even without a telescope, the eye can distinguish between large mare areas (dark) and highland or other mountainous areas of large extent (bright). The significance of these brightness variations, especially under full-moon illumination, has been an intriguing problem to astronomers for more than four centuries.

During the past 6–7 years, geologists have undertaken lunar albedo studies as a tool in mapping the lunar surface. Several relationships between reflected brightness and geology have been investigated in the lunar mapping program of the U.S. Geological Survey. Wilhelms (1966) noted that the brightness of some mare materials varies inversely with their age: the older—and more densely cratered—the mare, the higher its albedo. Before this relationship had been stated, however, differences in albedo had been used to divide the mare area and to establish superposition relationships in mare areas (Shoemaker and Hackman, 1962). The bright ray materials, whose radial patterns are so strikingly displayed under full-moon illumination, were notable examples of candidates for such analysis. Relative ages of crater ray patterns as well as other albedo patterns of mare units were thus delineated. As a result of photoelectric studies, Wildey and Pohn (1964) noted a general correlation between brightness of probable impact craters and their age: the younger the crater, the brighter its appearance. This inverse relationship (in comparison with the maria) may depend in part on the fact that larger areas of relatively light shock-metamorphosed material will be exposed in younger craters than in older degraded ones. Much more work is needed to determine how and to what extent geology correlates with albedo on a moon-wide scale.

While variation in reflective brightness is an important characteristic of the appearance of surficial materials during all phases of the moon, it is inseparable from topographic expression except when the phase angle is close to zero (during the full moon). The geometry of the general case is shown in figure 1. At full moon, when no shadows are visible from earth, the distribution of reflectivity appears to express actual variations in the composition or surface characteristics of the lunar surface materials. The diffuse reflectivity of the full moon is commonly expressed as normal albedo—the brightness of the lunar surface divided by the brightness of a Lambert surface when observer and light source are along the same normal vector. A Lambert surface is an ideal diffuse reflecting surface; it is nonabsorbing and uniformly bright from any viewing direction. (For more details see section on "The theory of Lambert scattering and the absolute calibration of normal albedo.") Because the reflectivity of the moon appears to be independent of the incident and emergent angles at zero phase angle (at least for terrestrial observations), the measured geometric albedo [1] at zero phase angle can be equated with the normal albedo, even though, as formally defined, they do not coincide at the subearth point.

NOTE.—In other words, the brightness exhibited by the lunar surface when sun, earth, and moon are alined (idealistically avoiding eclipse) is the same whether the lunar surface is oriented perpendicular to the line of sight or oriented in any

[1] Geometric albedo is defined in association with a Lambert surface, as is normal albedo; however, the geometry is flexible and must be specified together with the numerical value of the geometric albedo to avoid ambiguity.

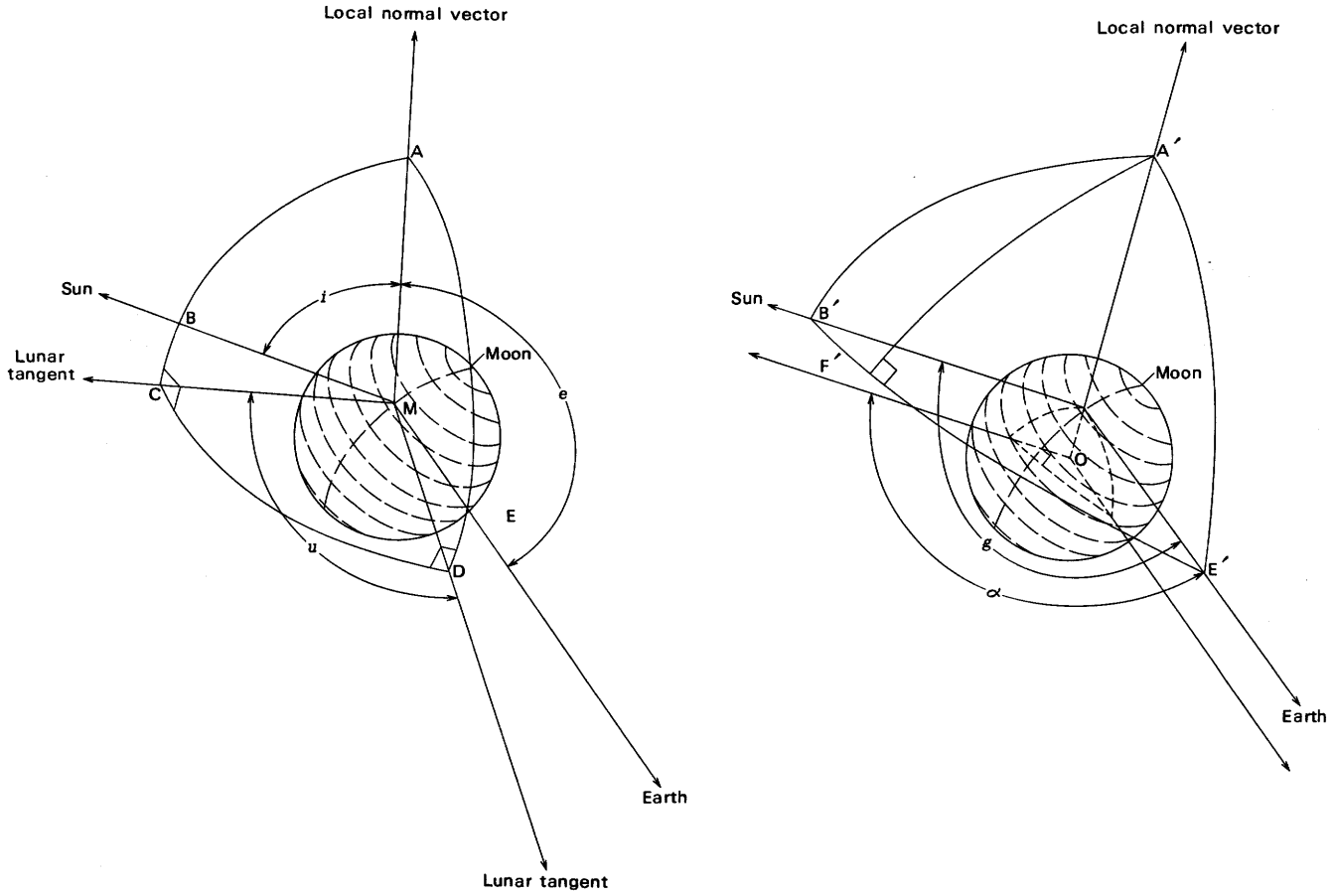

FIGURE 1.—Geometry of the generalized illumination and observation of the moon. An altazimuth coordinate system possessing no singularities is shown at left: $i \equiv$angle of incidence (of the sun), $e \equiv$angle of emergence (of the earth or wherever observation might be taken), and $u \equiv$azimuth between sun and earth. (Note that i and e are the complements of the local altitudes of the sun and the earth respectively.) On the right is a coordinate system having special significance for lunar reflectivity, which has a singularity at $g=0$; $g \equiv$phase angle; $\alpha \equiv$brightness longitude. A third coordinate seems to be unnecessary for specifying lunar brightness to present observational precision. That the directions to the sun (and the earth) are nearly parallel whether taken from the moon's center (shown as point O) or from any point on its surface is what characterizes α as a "longitude," assuming that the topography is flat. Full moon implies $g=0$.

other arbitrary way. Of course, the abrupt transition to zero brightness at an observing angle of 90°, beyond which forward scattering into an opaque medium would be indicated, must be smooth to avoid a physical discontinuity. However, the transition region occupies too small an angular range to be of concern here. The map resulting from the present study shows no obvious limb darkening with the possible exception of the extreme proximity of the limb. This constitutes one of the observational bases for the assumption that the photometric function of the moon has a value, at zero phase angle, which is independent of all other geometric degrees of freedom. The test is partly vitiated by the fact that the moon is not a body of uniform absorptivity.

There is a second observational basis for assuming that normal albedo and zero-phase albedo are equal. It is a fact, previously observed photoelectrically by the authors, that the brightness versus phase curves of a collection of 25 lunar features of various types and locations possess waxing and waning branches which coincide assymptotically near zero phase angle, regardless of location on the moon. Thus, for two small and equivalent phase angles (up to about 5°) taken before and after full moon, the value of the photometric function is the same even though changes in the values of the angle of incidence and the angle of observation may be as much as several degrees. This is, of course, a direct test of the assumption that the moon's zero-phase albedo is equivalent to its normal albedo. Unfortunately, the geometric limitations imposed by the moon's synchronous rotation and the earth-based nature of the observations do not permit a test in which the changes in observing and incident angles are a large fraction of their possible range.

A third basis is derived from the fact that previous studies have shown that the moon's photometric function depends predominantly, if not wholly, upon phase angle and brightness longitude, over the general range of variables. From the geometrical definition of brightness longitude, it can be easily shown that it is mathematically indeterminate at zero phase angle, hence the implication that it must approach zero influence in this neighborhood.

It thus appears that the assumption of the equivalence of normal albedo and zero-phase albedo rests upon a great deal of evidence. It is not fair to say, however, that the precision (over all the ranges of the variables involved) with which the assumption has been tested has been equal to the fundamental precision of the observational photometry, for the test of such an assumption appears to be fundamentally limited by the techniques of ground-based astronomy. Should practical consequences of the fact ever become significant, the authors wish to point out that the present study has produced a map of zero-phase geometric albedo whose approximation to a map of normal albedo is better than for which we can now test.

Photographic density can be measured on a full-moon photograph, but a map prepared solely by this method will show only isophotic patterns that cannot be directly or even proportionally related to normal albedo.

This lack of correlation to normal albedo arises from two sources. First of all, if the $D \log e$ curve is not obtained in any way whatsoever, contours of equal density will be isophotes whose relative brightness will be unknown and also variable as one goes from higher to lower densities, inasmuch as there is not a linear relationship between density and brightness. If the $D \log e$ curve is obtained from the imprint of a wedge or a spot photometer, one will obtain relative brightnesses devoid of systematic errors only if (1) the exposure times used in the lunar and calibration photography are the same to within approximately 50 percent and (2) the radiative energy distributions of the moon and the calibration source agree to within a few tens of percent. The imprinting process must also be known to be devoid of errors.

Second, absolute calibration by purely photographic means requires an absolutely standard comparison source whose image is processed in a rigorously equivalent manner. If errors due to atmospheric transmission fluctuation are avoided, the standard should be extraterrestrial, preferably near the moon. In general, if the spectral energy distributions of moon and standard are not exactly the same, the spectral responsivity of the emulsion must be known. Thus to relate photographic density to normal albedo, it is helpful to make true radiative power measurements external to the plate. Even calibration in this manner is not possible, however, unless care is taken to insure uniformity of exposure, emulsion sensitivity, and development.

Most early lunar photometric observations were purely photographic (Minnaert, 1961). The advantage of a photographic plate is that all image elements [2] in the brightness distribution of a celestial body can be observed simultaneously. On the other hand, the photoelectric technique, although it can only record one image element at a time, produces a recorded signal which is linear in specific intensity (equivalent to surface brightness), extremely precise, highly stable, and easily calibrated to absolute units. Unfortunately, individual resolution elements of the picture must be recorded consecutively by some form of spatial scanning. This is time consuming and can lead, under certain conditions, to spurious brightness variations in the image because of the fluctuations with time in atmospheric transmission.[3] Clearly, one way to obtain reliable photometric measurements of the entire full-moon disk is to use a photoelectrically calibrated photograph.

Obtaining reliable photoelectric and photographic data on the full moon presents several problems. For the best photoelectric data, the sky must be absolutely cloud free and the minimum lunar phase angle must be small (1.5°–2.0°). Because of atmospheric transmission difficulties, the minimum phase must occur when the

[2] Image element is defined as the largest size of a measuring cell of the picture whose ensemble is capable of retrieving all the information that the picture contains. It is an element of resolution, in a sense; however, the term "resolution" is somewhat ambiguous.

[3] Of course the atmospheric transmission must change because the zenith angle of the moon changes. What is specifically referred to here is a fluctuation in the value of the atmospheric extinction coefficient.

moon is 30° or more above the local horizon.[4] Furthermore, astronomical "seeing" conditions should be reasonably good.

Although adequate photoelectric equipment has been available for some time, practicable means of controlling photographic parameters have not yet been fully developed. Such techniques as do exist are usually either time consuming or expensive and often not as adequate as specified. Although the photoelectric requirements appear more complex than other techniques, they can be met by taking straightforward measures. The proper means of solving the photographic problem presents subtle difficulties. There are two techniques for insuring uniform exposures. One employs a moderately fast emulsion coupled with a highly uniform motion of the shutter across the focal plane. The other employs a slow emulsion, hence relaxed shutter tolerances (a hand-pulled slide will suffice), coupled with very precise guiding of the telescope. The latter technique was used in this study.

Uniform development, an essential element in photometric photography, can be achieved in several ways. In one technique, the plate is inserted flush with the bottom surface of a square tray. The tray rotates about an axis normal to its bottom surface. This axis in turn is caused to precess about the local vertical of the earth, with which it makes an angle of about 10°. Another technique involves the periodic bursting of nitrogen gas into a developing solution in which the plates are mounted vertically. Although many plates can be processed simultaneously, not enough uniformity is achieved. Probably the slowest but best technique is to spread the developer by passing a very fine fiber brush back and forth across the emulsion surface; this was done in this study.

Uniformity of emulsion sensitivity is usually obtainable. Occasionally, however, the spatial responsivity of a shipment of 5- by 7-inch spectroscopic plates varies enough to cause systematic discrepancies of as much as 0.10 magnitude in stellar photometry. Such variations must, therefore, be monitored and, if necessary, corrected for. Such corrections have been unnecessary in the present study.

A preliminary version of the map developed in this study has been available for nearly 2 years. It has provided albedo data useful in the preparation of reconnaissance maps of lunar quadrangles, has been a primary source of engineering data contributing to the successful performance of lunar missions, and has provided data for shutter settings of the Lunar Orbiter cameras.

Acknowledgments.—Many individuals assisted in the collection and reduction of the data. The authors are particularly grateful to Harold Ables, who exposed and processed the plates, Dr. G. E. Kron, Director of the Flagstaff Station of the U.S. Naval Observatory, who permitted use of the 61-inch telescope for data collection purposes, J. J. Woolridge, of the U.S. Geological Survey, who supervised the plate reduction on the Isodensitracer, and R. E. Sabala, R. D. Carroll, L. J. Wester, C. E. Hazelwood, and J. W. Van Divier, who compiled and contoured the map.

THE OBSERVATIONS

On the night of June 2–3, 1966, a 45-second exposure of the full moon was taken at the folded prime focus of the 61-inch astrometric telescope at the U.S. Naval Observatory's Flagstaff Station in Arizona (fig. 2). The phase angle at the time of the exposure ($07^h07^m05^s$ u.t.) was 1.52°. An Eastman Kodak 649 F emulsion was used, preceded in the focal plane by a 2.0-millimeter-thick Schott GG 14 filter. The spectral response of the filter plus emulsion did not correspond exactly to the photoelectric visual band, but lunar surface color variation is too small to require correction. The plate was brush developed in ultra-fine-grained developer diluted one to one with water for 6 minutes to insure highly uniform development. The manufacturer's preparation of the original emulsion was highly uniform. The overall uniformity (including all sources of random error and any errors systematically dependent on location upon the lunar disk) is well represented by the degree of scatter in the calibration plots of this study because of the wide distribution of calibration points over the lunar surface.

The photoelectric observations were made by the authors on the night of June 2–3, 1966, concurrently with the photographic observations. The 30-inch reflector of the U.S. Geological Survey observatory on Anderson Mesa, about 15 miles from the Naval Observatory and at about the same elevation, was used. Four scans were completed. Although the seeing was only fair, the seeing tremor disk was much smaller than the aperture size of the diaphragm utilized in the photometer. The photoelectric photometer used was designed by the authors (figs. 3, 4). It employs a thermoelectrically cooled RCA 1P21 photomultiplier in combination with a Wratten 8 filter to produce a close first approximation to the visual bandpass used in the Johnson-Morgan *UBV* system (Johnson and Morgan, 1953). A periscope allows manual telescope tracking corrections during measurement. The blue bandpass employs a filter consisting of 1.3 mm

[4] The atmospheric transmission, from an information-theoretical point of view, is a source of nonstationary noise. The fluctuation of atmospheric extinction is neither random nor predictable for practical observing durations. Consequently, the larger the extinction correction, the larger the error of its determination. The practical limit for 1 percent accuracy is about 30°.

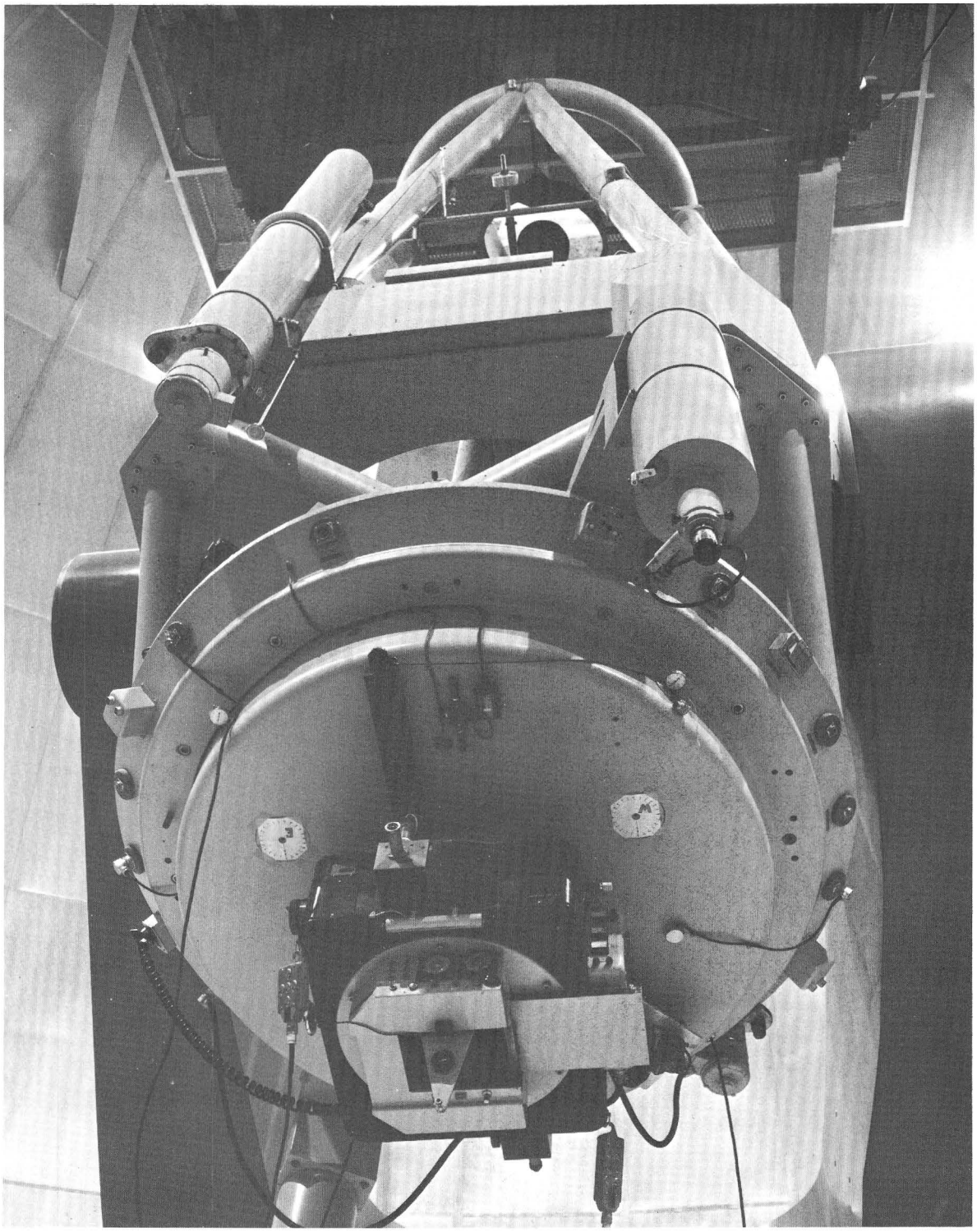

FIGURE 2.—The 61-inch *f*10 astrometric reflecting telescope with direct photographic camera used to collect the photographic plate data for the albedo map obtained in the present study. Folded-prime focus is behind primary mirror as in Cassegrain systems. A swing-out position-finding eyepiece is shown at bottom. The plateholder fits into slot immediately behind this eyepiece. The side-mounted eyepiece near the top of the black module immediately behind the primary mirror cell is for manual telescope guiding. The rest of this section contains the automatic photoelectric guiding. Auxiliary telescope facilitates position finding. (Photograph by U.S. Geological Survey through the courtesy of U.S. Naval Observatory.)

373-263 O—70——2

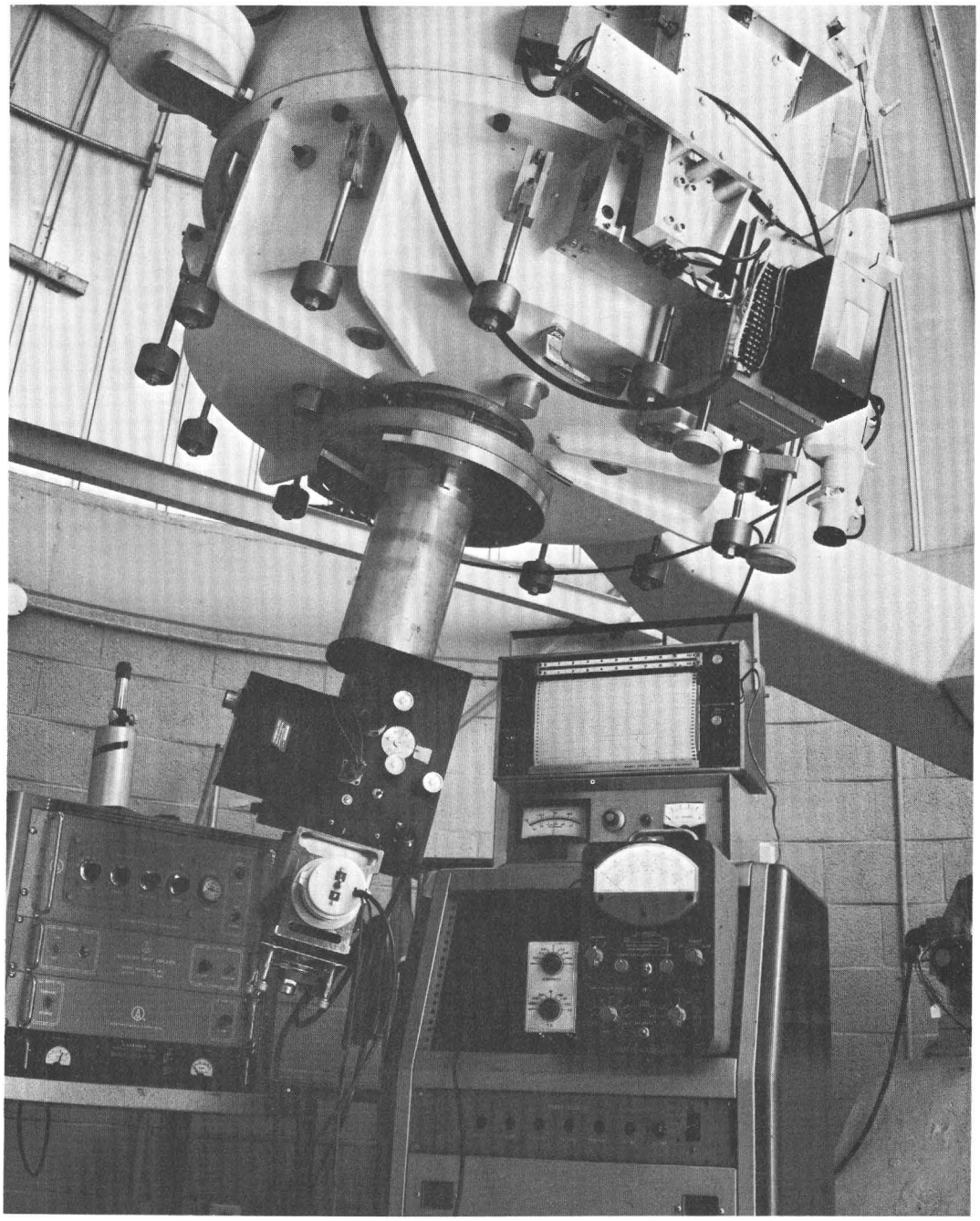

FIGURE 3.—U.S. Geological Survey 30-inch *f*15 Cassegrain telescope with photoelectric photometer attached to tailpiece; this equipment was used to obtain the photoelectric observations for the albedo map of the present study. The electronics bay on the left houses the power supply, oscillator, and amplifier for the variable hour angle drive of the telescope. A variable declination drive is not shown. The photometer is displayed with three prominent sections. Lowermost is the Frigitronics cold-box housing the 1P21. Thermoelectric cooling is used, with styrofoam insulation. Heat is carried away from the cooling fins by an electric fan. In the middle is the optics section, containing filter wheel, focal-plane-diaphragm wheel, and knife-edge focus viewer. The box on the immediate left side contains a periscope for viewing the focal plane image. From top to bottom in the electronics bay to the right of center, is seen a Mosely Autograf strip chart recorder, a Frigitronics thermoelectric current generator, and a General Radio Direct-Current Amplifier and Electrometer. Farther down and out of the picture is a Calibration Standards high voltage power supply that is set at 900 volts; it supplies the photomultiplier bias. A Sorenson voltage regulator is the main power source for the bay.

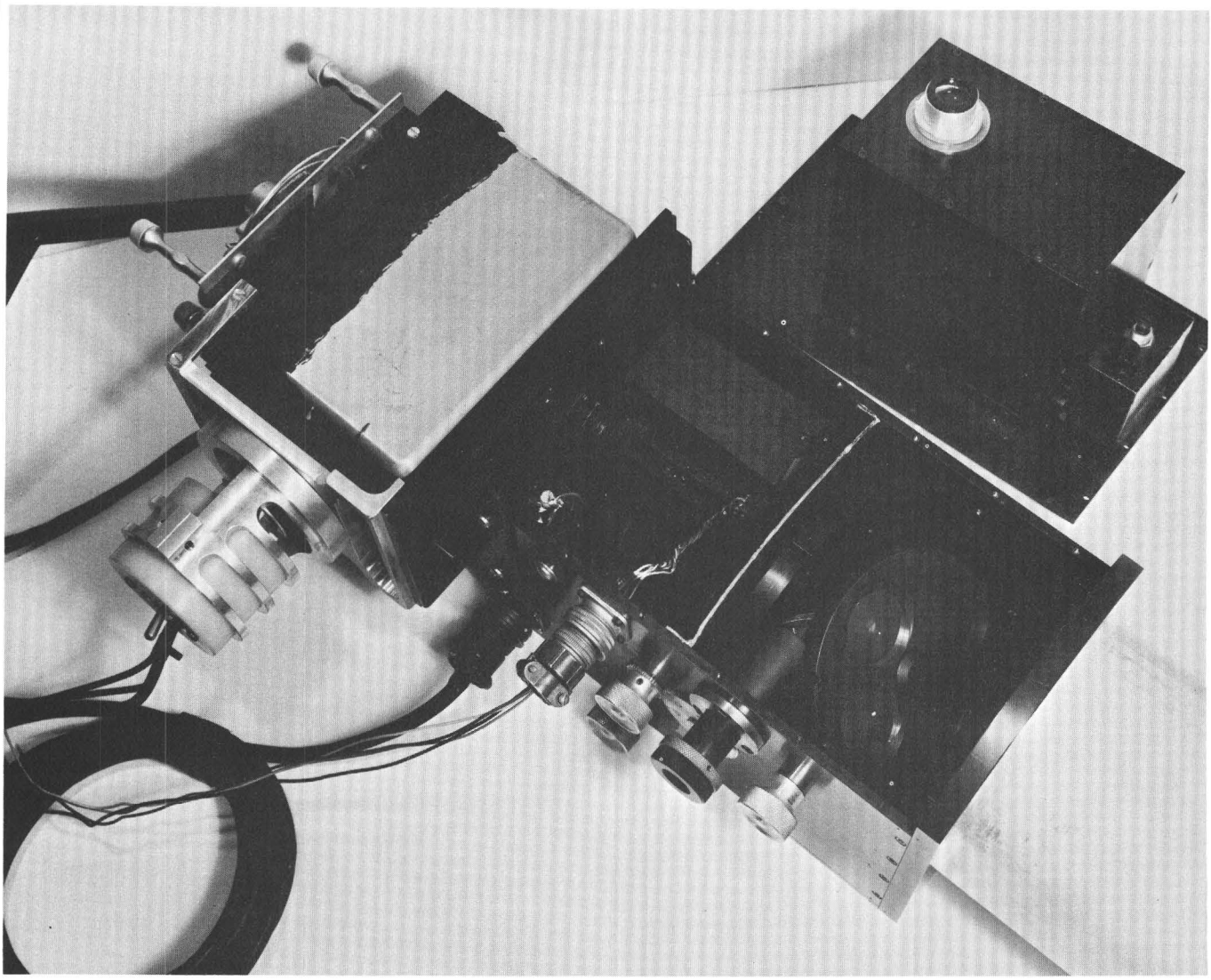

FIGURE 4.—Photoelectric photometer with periscope viewer removed to reveal the internal workings. The light from the telescope enters from the lower right-hand corner. The wheel angled at 45° to the optical axis has selectable aluminized diaphragms with variable sized apertures. The focal plane is formed at the center of the aperture. A large aperture is used for stellar measurement, and the smallest for lunar measurements. The periscope thus views the lunar image with a dark spot signifying the portion of light admitted to the photomultiplier. Immediately behind this wheel is a plunger-operated periscope which, when "in," provides a view of that part of the focal plane within the aperture. Since one of the positions on the wheel is a knife edge, the focusing of the telescope is also facilitated at this viewing port. In the "out" position, light is allowed to pass into the balance of the photometer. Next, the wheel that is perpendicular to the optical axis houses fix filters, three of which are now kept opaque and three of which contain the *UBV* filters. Behind this wheel is a partition with a filter-size aperture for reduction of the admission of scattered light into to cold-box. A rotating polarimeter which can be inserted into the light path via a plunger-operated slide was not used in this study and is shown at the far side (upper right) of the section behind the partition. On the upper left wall of this section may be seen the Fabry lens (quartz) which focuses an image 0.25 centimeters in diameter of the primary mirror on to the photocathode of the 1P21. The toggle switch at the side of the cold-box enables the selection of either the standard 10 dynodes of multiplication or, through short circuiting the last stage, nine dynodes and a double anode. In this way the linear range of the photomultiplier is extended by postponing space-charge limited operation without the problem of the gain instability that would attend the accomplishment of the same end by lowering the supply voltage.

of Schott GG 13 and 0.7 mm of Schott BG 12. The ultraviolet filter is a Corning 9863. The focal-plane diaphragm transmits a circular beam of light 2.64″ of arc in diameter corresponding to a spot 4.8 kilometers across at the center of the lunar disk.

The photographic data were reduced on the Joyce-Loebl microphotometer—Beckman and Whitley Isodensitracer (IDT) combination using a square aperture 0.173 mm on a side. This aperture setting resulted in a sampling resolution for the photographic plate that was comparable to the resolution inherent in the spatial scans made with the photoelectric photometer at the telescope. It is also consistent with the maximum amount of information that can be portrayed on a 1:5,000,000-scale map, even though the plate can yield additional information at finer sampling resolution.

The interval between scan centers on the plate was 75μ and provided an overlap of 57 percent between successive scans. The calibration wedge used in the IDT had a dynamic range of 0–2.4 in optical density, with step increments of 0.1195 in density. The range of normal albedo was thus divided into 20 unequal contour intervals. The maximum (23 percent) and minimum (7 percent) values of the moon's normal albedo have been satisfactorily bounded by the scale.

ABSOLUTE CALIBRATION

Of the four photoelectric scans taken on the night of June 2–3, one scan of the southern lunar highlands was rejected because its location could not be precisely determined, and a second scan taken centrally on the disk was rejected because a large atmospheric extinction correction was required. The two remaining scans, one near the equator and the other at about lat 25° N., were taken immediately before and after the photographic plate was exposed. Scanning time was approximately 25 minutes per scan; each extended from limb to limb. To insure coverage of the extremes of brightness of the lunar disk, single points in Aristarchus, Tycho, and Le Monnier were also measured.

For precise calibration the requirements were a selenographic congruence of points measured both photoelectrically at the telescope and densitometrically on the lunar photograph. The photographic plate was positioned on the IDT (operating in the scan mode) to reproduce exactly the selenographic traverses of the scans which were obtained by the photoelectric photometer directly at the telescope (fig. 5). In addition, densities of the control points in Aristarchus, Tycho, and Le Monnier were individually measured on the plate.

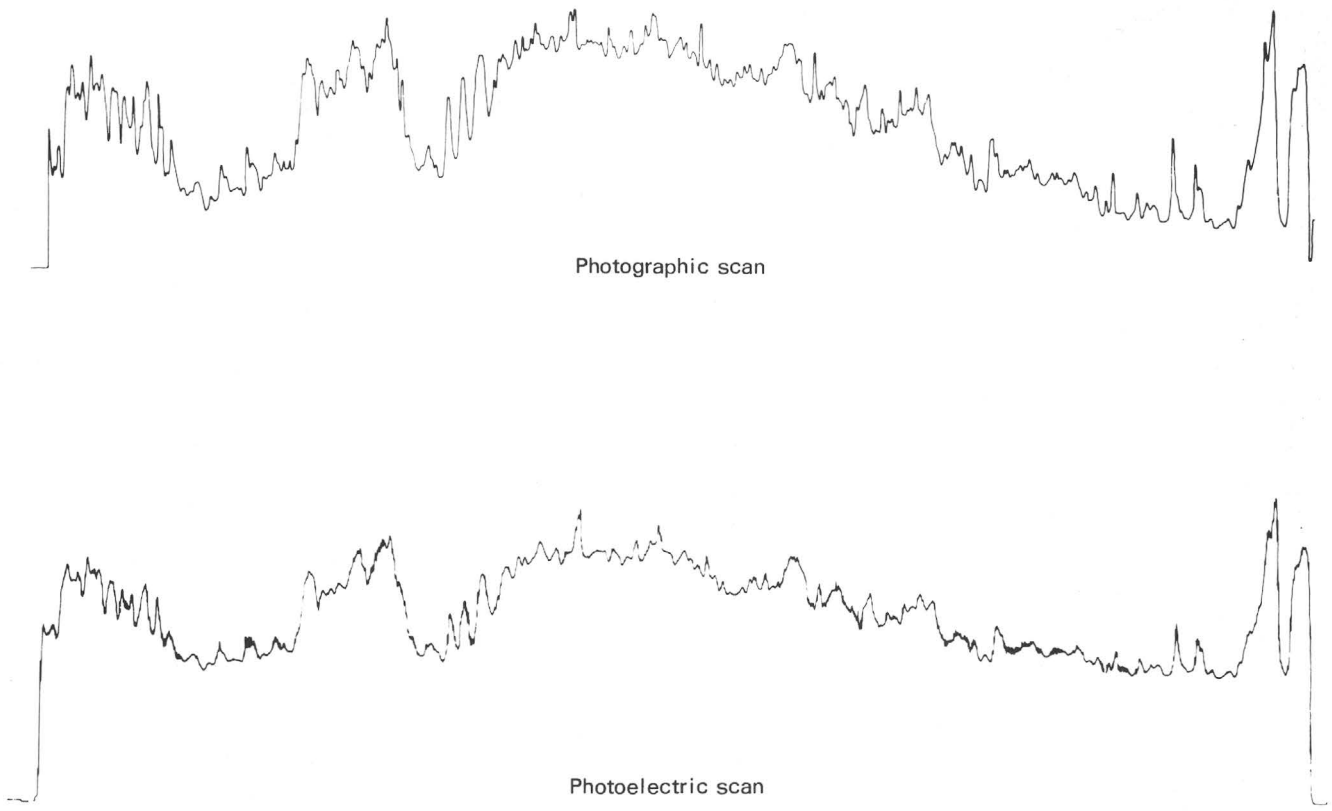

FIGURE 5.—A comparison of signal traces adjusted to the same scale of abscissa. Both follow the same track across the moon. Lower curve: amplified photoelectric voltage as ordinate on the same voltage scale used for recording flux voltages of standard stars. Upper curve: continuous record of density of the simultaneously recorded photographic plate on the same vertical density scale that is coded by the Joyce-Loebl—Beckman and Whitley Isodensitracer.

It is most convenient to convert the signal scale of the photoelectric charts to normal albedo before relating the photoelectric photometry to the photography. Determination of normal albedo from photoelectric signal proceeds in three steps (for more details see specified sections in "Conversion and calibration data"): (1) Correction of the photometry for differences in spectral response and power scale between the operational system of the telescope-photometer (after correcting for atmospheric extinction) and an intermediate standard system, in this case, the Johnson-Morgan *UBV* system (see section on "The theory of astronomical photometry and systems of stellar magnitudes and colors"); (2) conversion of the intermediate *V* magnitude to a wavelength-averaged absolute specific intensity or surface brightness (see section "The theory of Lambert scattering and the absolute calibration of normal albedo") and a corresponding effective wavelength (see section on "Specific intensity and effective wavelength"); (3) determination of the normal specific intensity of a Lambertian scattering surface at the same distance from the sun on the basis of published absolute solar photometry (see section on "The theory of Lambert scattering and the absolute calibration of normal albedo").

A small correction (0.05 magnitude), obtained from the brightness versus phase curves at small angles (Wildey and Pohn, 1964), was applied to extrapolate magnitudes to zero phase angle. Within about 5° of zero phase angle, variation in size of the extrapolation does not correlate with class of lunar feature (within the precision of the investigation), and the waxing and waning branches of the brightness versus phase curves coincide regardless of selenographic coordinates. This asymptotic coincidence demonstrates the mathematical degeneracy of the photometric function, in the neighborhood of zero phase angle, in all its geometric degrees of freedom except phase angle. This degeneracy is of course essential to the labeling of the full-moon photograph with values of normal albedo, because the phase angle is the only geometric degree of freedom in the photometric function which is reasonably constant over the entire moon.

Photoelectric voltages are scaled to normal albedo in the following way. The ordinate of the photoelectric trace in the lower part of figure 5 is linear in the number of photons received per second and thus linear in specific intensity and normal albedo. The zero point on the trace (corresponding both to zero photoelectric voltage and zero normal albedo) is determined by the signal of the adjacent sky, which is negligible compared with that of the moon. The hypothetical full-scale signal of the yellow trace, together with a blue signal obtained from an independent photoelectric measurement of ratio of blue to yellow signals—reasonably the invariant over the lunar disk—can therefore be reduced to obtain, in sequence, a *V* magnitude, a specific intensity, and a normal albedo for a full-scale deflection. With these limits of normal albedo, the rest of the scale follows by a direct proportioning over the ordinate interval.

By obtaining absolute spectral radiometry on any one of the *UBV* standard stars, or any nonvariable star whose *V* magnitude and *B–V* color index will at some time be determined by photoelectric measurement, an absolute calibration of the entire *UBV* system can be determined. Such data were collected by Willstrop (1960), and the resulting calibration was determined by Wildey and Murray (1963). The conversion from a *V* magnitude of a known solid angle to a specific intensity can thus be obtained.

In the determination of normal albedo from observed specific intensity, a hypothetical Lambert surface must be placed at the point in space occupied by the moon, and the specific intensity that it would exhibit because of its diffuse reflection of sunlight must be calculated. The distance from the sun to the earth-moon system at the time of the observations is obtained from the ephemeris. A hypothetical Lambert scattering surface has a specific intensity under normal illumination which is completely specified by the properties of (1) total reflection, (2) a specific intensity constant over all positive directions and zero over all negative directions, and (3) a known apparent *V* magnitude for the sun (Stebbins and Kron, 1957). An observational normal albedo is obtained by dividing the observed specific intensity by the calculated specific intensity of the Lambert surface.

Once a normal albedo scale had been established for the photoelectric photometry, the next step was to determine its relationship to photographic density. The maximums and minimums of the curves obtained from the photographic and photoelectric scans (fig. 5) were intercompared, and a calibration plot (fig. 6) was constructed using the density values from the photographic plate and the absolute albedo values obtained from the photoelectric photometry. The choice of the extrema of the scans as calibration points was based on the assumption that the necessary geographic correspondences would thereby be assured. Several values near the limb were rejected owing to the severe positional effects in limb regions of the differences in lunar libration between the time of the photographic exposure and the times of the photoelectric measurements. The point plot for the calibration curve shows the maximum possible random error, since the extremes of the signal traces are most likely to be subject to errors due to astronomical

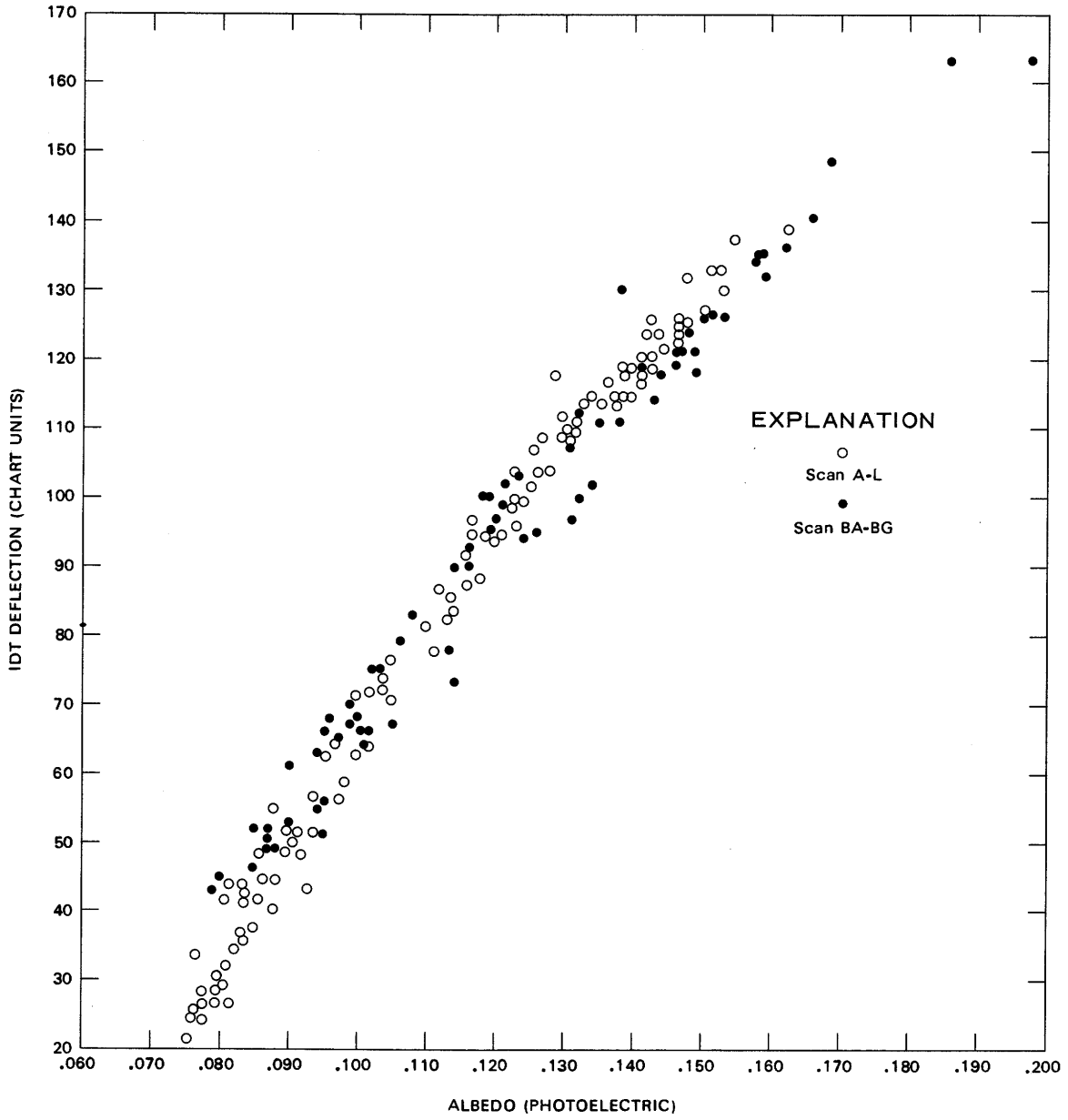

FIGURE 6.—Calibration plot of points on the moon measured simultaneously by photoelectric photometry and photography. Corresponding maximums and minimums of the photoelectric and photographic spatial scans from figure 5 were used.

"seeing" and any residual positional inaccuracy. The magnitude of the scatter about the calibration curve implies a nominal error of about ±1 percent.

THE ABSOLUTE ALBEDO MAP

One major departure from standard mapping procedure was used in constructing the absolute albedo map, and a brief explanation of this departure will enable the reader to better utilize the data. The contour intervals as recorded by the isodensitracings of the full-moon plate are constant in photographic density but not in albedo (see fig. 6). This is an unavoidable limitation in the present operation of the IDT. Despite this, the authors felt that the labeling of contours by albedo would be more practical than the imprinting of optical density, which would require frequent reference to the calibration curve.

For the albedo map to be used to maximum advantage, it must be understood that the quantization interval of the IDT is not sufficiently small to permit an adequate linear interpolation between contours in all cases. The print of the photographic plate (see pl. 1)

should therefore be used as an interpolation device. As an example of an associated problem, contacts between different types of lunar surficial materials will not always be demarcated by a contour line. The IDT shifts operational mode at predetermined equal increments of density. Therefore, if the machine is set to change mode at density increments corresponding, at a certain level, to 5 percent variation in surface brightness, a contact corresponding to a 3 percent brightness change, at that level, may or may not show on the tracing because it might conceivably be contained entirely within one contur interval, depending on the arbitrary zero point of the density encoding process. An example is shown in figure 7. The area measured is in Mare Serenitatis. In figure 7*A*, the setting of the zero point of the machine fortuitously caused the mode switch to be correlated with the border of dark materials which surround Mare Serenitatis (fig. 8). In figure 7*B*, the zero point was shifted slightly, and thus the contour lines no longer have geologic significance in this region. The effect is subtle in that the border pattern, which appears in both, is the proper size to coincide with the contact in only one case.

Areas with extremely steep brightness gradients present another problem. When the IDT reaches an area of large change in brightness over an interval which is small with respect to the aperature, the finite speed of the plate carriage forces the IDT to change modes as rapidly as it can. The contours in a small bright region, therefore, will tend to assume a symmetrical shape even if the true brightness configuration is actually asymmetrical.

In summary, this is the first reliable map of the absolute normal albedo of the moon in which real-time photoelectric calibration is utilized and for which the necessary uniformity in plate parameters is known. The map is, however, considered provisional in three aspects: (1) The absolute scale of normal albedo may undergo a blanket correction factor of a few percent difference (relative) from the present data owing to a refinement in absolute calibration presently under study. This will not affect an albedo reading at a point on the map if it is considered as a ratio to a reading at some other point on the map. (2) The brightness gradients of very small bright lunar features, such as some bright halo craters, were too steep for the IDT to follow, and the peak values indicated are too low by an uncertain amount. (3) In a broader sense, additional information can be obtained from the photographic plate by increasing the number of contour intervals and sampling with a narrower aperture setting on the IDT. This is warranted by the "seeing" conditions that existed when the plate was exposed but can be realized only by mapping at a larger scale.

REFERENCES

Carr, M. H., 1966, Geologic map of the Mare Serenitatis region of the moon: U.S. Geol. Survey Misc. Geol. Inv. Map I–489.

Johnson, H. L., 1955, Spectral responses of a precisely transformable two-color system which excludes the Balmer jump: Annales Astrophys., v. 18, p. 292–295.

Johnson, H. L., and Morgan, W. W., 1953, Photometry of 290 stars in three colors: Astrophys. Jour., v. 117, p. 313–323.

Minnaert, M. G. J., 1961, Photometry of the moon, Chapter 6 *in* Kuiper, G. P., and Middlehurst, B. M., eds., Planets and and satellites, Volume 3 *of* The solar system: Chicago, Univ. Chicago Press, p. 213–248.

Shoemaker, E. M., and Hackman, R. J., 1962, Stratigraphic basis for a lunar time scale, *in* Kopal, Zdenek, and Mikhailov, Z. K., eds. The moon—Internat. Astron. Union Symposium 14, Leningrad 1960: London, Academic Press, p. 289–300.

Stebbins, Joel, and Kron, G. K., 1957, Six-color photometry of stars; X, The stellar magnitude and color index of the sun: Astrophys. Jour., v. 126, p. 266–280.

Wildey, R. L., and Murray, B. C., 1963, Ten micron stellar photometry—First results and future prospects: Colloque Internat. d' Astrophys. tenu a l'Univ. de Liege, 24–26 juin 1963, v. 26, p. 460–468.

Wildey, R. L., and Pohn, H. A., 1964, Detailed photoelectric photometry of the moon: Astron. Jour., v. 69, p. 619–634.

Wilhems, D. E. 1966, Summary of telescopic lunar stratigraphy, *in* Lunar and planetary investigation, Part A *of* Astrogeologic studies annual progress report, July 1, 1965 to July 1, 1966: U.S. Geol. Survey open-file report, p. 235–298.

Willstrop, R. V., 1960, Absolute measures of stellar radiation: Royal Astron. Soc. Monthly Notices, v. 121, p. 17–26.

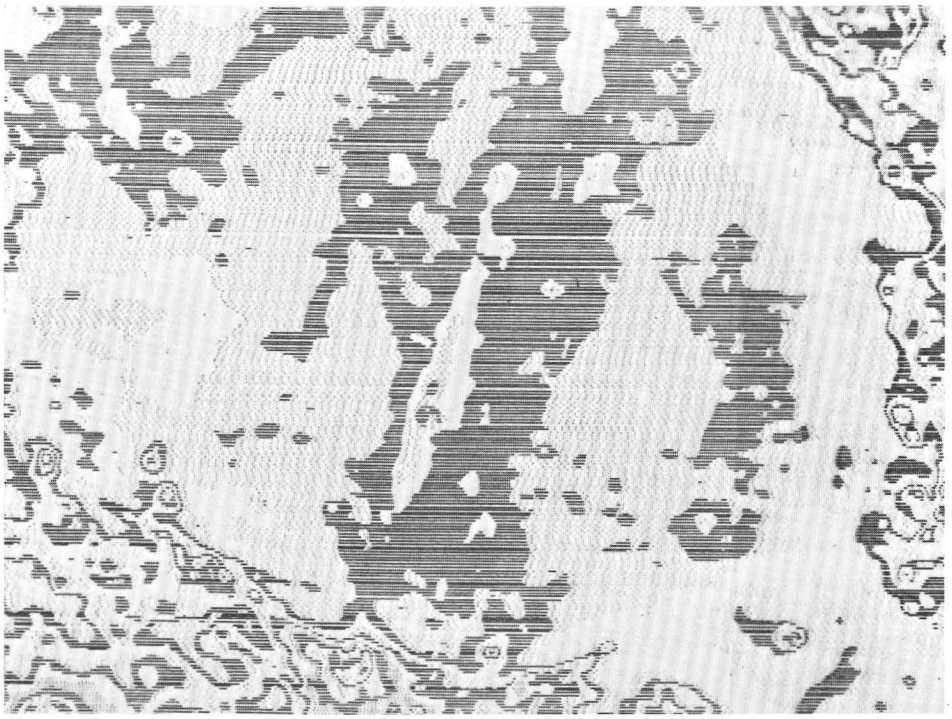

A

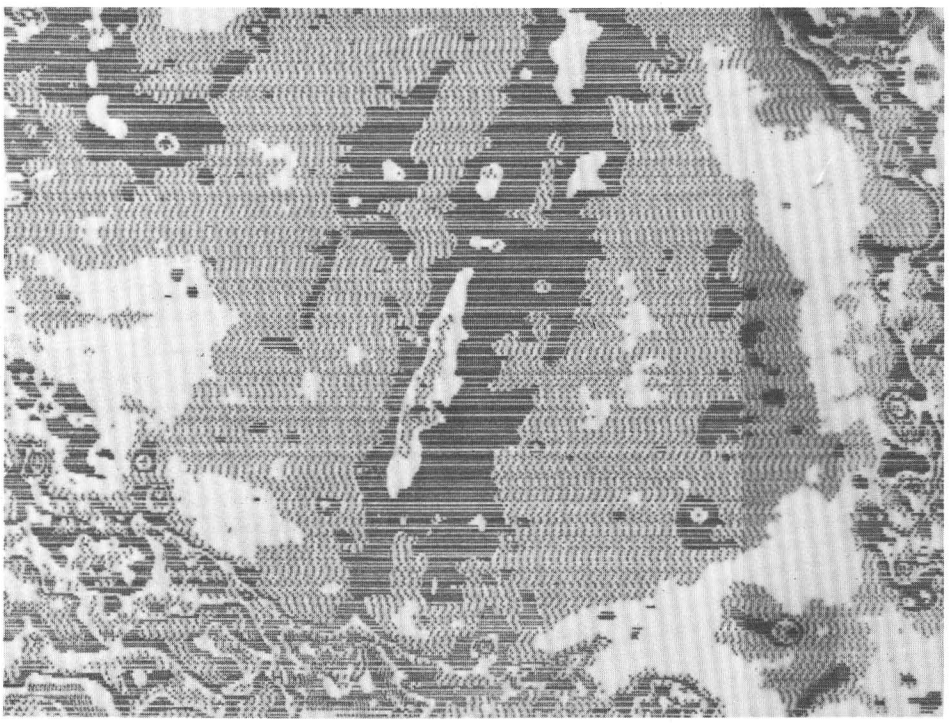

B

FIGURE 7.—Isodensitracings made from the photographic plate used in the present lunar photometry. *A*. Contours corresponding to areas of geologic significance. *B*. Contours showing no geologic significance.

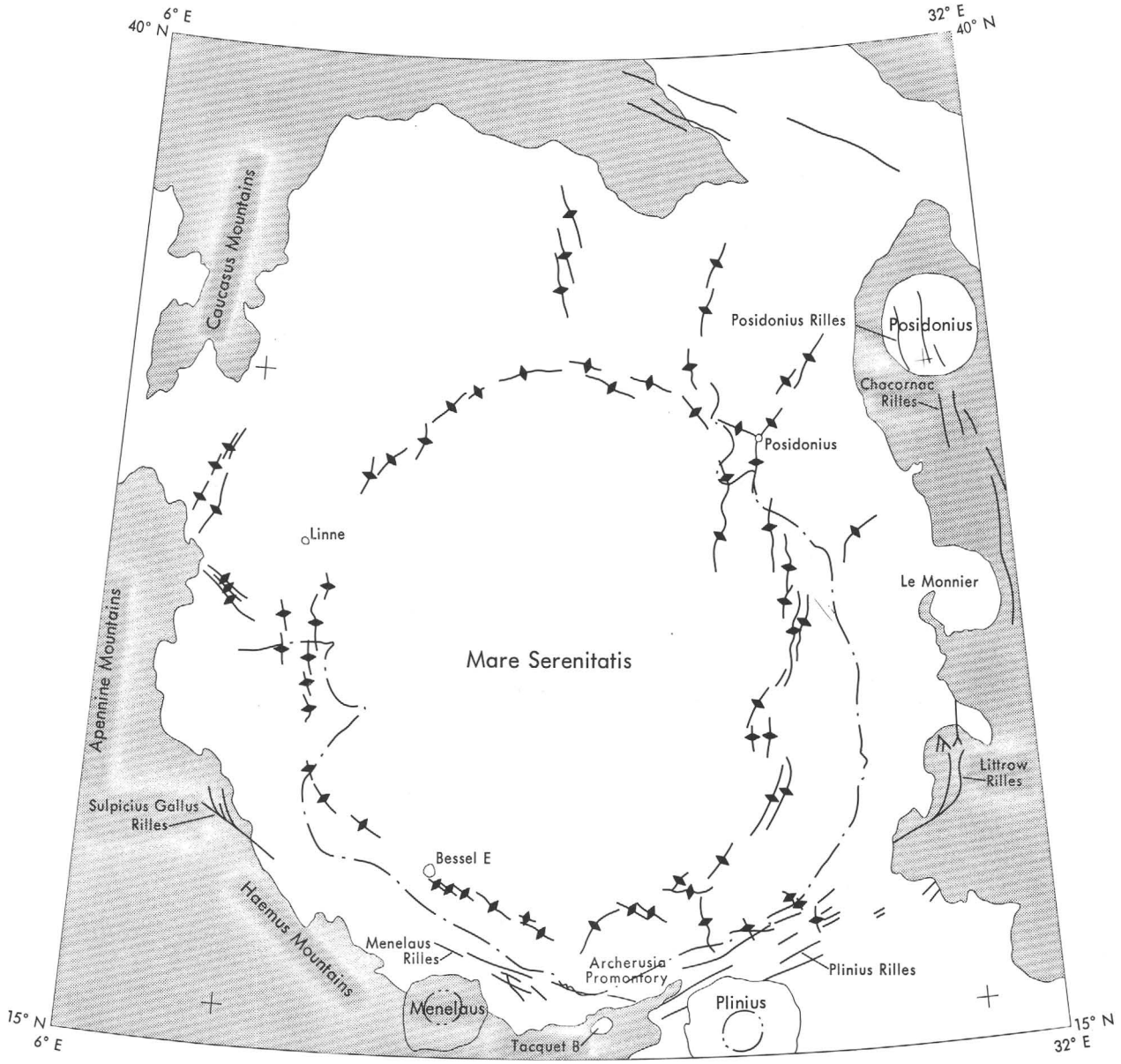

FIGURE 8.—Sketch of Mare Serenitatis showing extent of dark mare unit (dashed and dotted line). Stipple indicates terra. Ticks near lower right- and left-hand corners indicate corners of geologic map of region (Carr, 1966). Scale 1 : 5,000,000. Lines with diamond-shaped smybols indicate mare ridge.

CONVERSION AND CALIBRATION DATA

SPECIFIC INTENSITY AND EFFECTIVE WAVELENGTH

Specific intensity is the most general parameter associated with a radiation field. It is the one from which all others (for example, mean intensity, flux, radiation pressure) are derivable, and it is defined in the following way: Consider a truncated cone where the apex angle of the fully extended cone defines a solid angle and the truncating cap defines an area. Measure the radiative power for all photons which pass first through the truncating cap and then through the base of the cone; divide by the product of the area of the cap and the solid angle of the cone. In the limit as the cone angle approaches zero, the quantity so defined is the specific intensity. The following equations show the mathematical relations between quantities defined in the text and figure 9 for unit time interval.

$$I=\frac{\Delta \text{ Energy}}{\Delta A \cdot \Delta \Omega}$$

$$I'=\frac{\Delta \text{ Energy}}{\Delta A' \cdot \Delta \Omega'}$$

$$\Delta A'=\Delta \Omega(381{,}000)^2$$

$$\Delta \Omega'=\Delta A/(381{,}000)^2$$

$$\therefore I'=I$$

Specific intensity is characterized by a direction and is measured in watts per square centimeter (of area normal to the direction) per steradian (of solid angle surrounding the direction) per unit wavelength (if not bolometric). As mathematically shown above, specific intensity does not vary with distance in a nonabsorbing medium. If not bolometric, it may be truly monochromatic or an average associated with some broad spectral response function. In the latter case, it can be associated with an effective wavelength. At lease two kinds of effective wavelength can be defined, the most meaningful of which is probably

$$\lambda_e=\frac{\int_0^\infty \lambda I_\lambda R_\lambda d\lambda}{\int_0^\infty I_\lambda R_\lambda d\lambda},$$

where

λ=wavelength,
I_λ=specific intensity, and
R_λ=spectral response of photometer.

The effective wave length for the present observations is approximately 5,540 A (angstroms).

That the number of photons per second registered by the photometer is directly proportional to specific intensity may be realized as follows (see fig. 9): The radiative power accepted originates in an area of lunar surface corresponding to the fraction of image encircled by the aperture in the focal plane diaphragm. The size of this area, as direction away from the surface varies, accommodates itself so that the projection of this area onto a plane perpendicular to the line of sight remains fixed in size for a given earth-moon distance. Furthermore, the photons originating in this area are constrained to travel on rays within the solid angle subtended at the moon by the telescope objective. If the earth-moon distance is changed, the diminution of solid angle is exactly compensated by the increase in the geographic area of the moon being measured. The signal will thus remain unchanged if resolution is not a consideration, in which case the solid angle and the area considered are small enough to be considered as mathematical differentials. Their product, which would be divided into the signal, is thus a constant. Hence, the signal is proportional to specific intensity.

THE THEORY OF ASTRONOMICAL PHOTOMETRY AND SYSTEMS OF STELLAR MAGNITUDES AND COLORS

Normally, standards of celestial photometry are established by measuring a collection of stars of constant luminosity over a period of time during which equipment response parameters can be kept constant. The photometric investigation of other objects (undertaken at arbitrarily later times), when coordinated with the measurement of some of these standard stars on the same nights, can then be rendered on a highly homogenous photometric system. Extremely accurate comparison with other objects measured in the same way is possible because corrections can be made not only for (1) the nightly deviation of the average atmospheric extinction from the secular average used in the reductions and (2) the uncertainty in the bolometric responsitivity of a given photometer, but also for (3) small color deviations in the spectral response characteristics of a given photometer from those of the original photometer used to establish the collection of standard stars. To do this, the photometry must be at least two-color (in two different wavelength bands).

The reduced form of stellar photometry is on a logarithmic scale. The flux measurement is given as a "magnitude," and the colorimetry (magnitude difference) is a "color index." The unit, or zero point of the magnitude system, is essentially arbitrary though it stems ultimately from the naked-eye observations by Aristarchus of Samos, whose brightest stars were "stars of the first magnitude." Although the original reason for a logarithmic scale was physiological, a more scientific

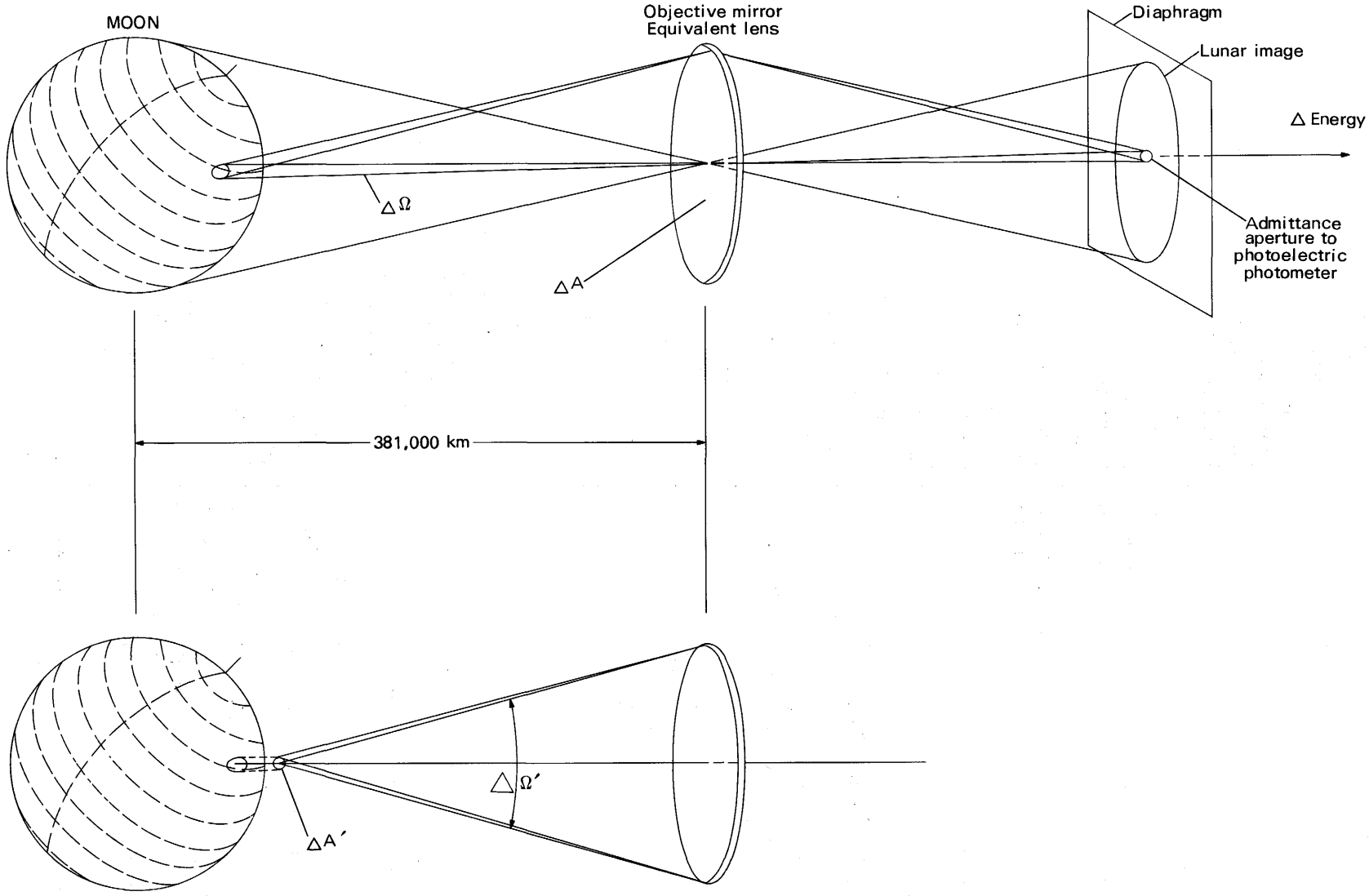

FIGURE 9.—Optical schematic diagram of the unfolded geometry relating the photoelectric photons captured to their origin on the moon's terrain. Two equivalent views of the transduction process are shown. They define the distance-independence of specific intensity and relate specific intensity to point-source fluxes. Peripheral beams as well as the beams on the optical axis are shown in each view. The locus of such beams over the areas shown in each case yields the total radiative power.

rationale can now be developed for its preservation.

Consider the monochromatic radiation of a blackbody at four different wavelengths. Let us then define four monochromatic magnitudes as follows:

$$m_j=-2.5\log\left[\frac{1}{\lambda_j^5(e^{hc/\lambda_j kT}-1)}\right].$$

The expression on the right is the Planck function multiplied by a convenient constant which need not concern us since the zero point of the m_j magnitude is arbitrary, needing only to be preserved after once being chosen.

For stellar temperatures and the wavelengths of ordinary photometry, Wien's approximation holds; hence

$$m_j=12.5\log\lambda_j+(2.5\log e)\frac{hc}{\lambda_j kT}.$$

Color indices are, for a given T,

$$m_i-m_j=12.5\log\frac{\lambda_i}{\lambda_j}+2.5\frac{hc}{k}(\log e)\frac{1}{T}\left(\frac{1}{\lambda_i}-\frac{1}{\lambda_j}\right).$$

By writing down the foregoing equation for i, $j=1$, 2 and again for i, $j=3$, 4, one can readily solve simultaneously for the relationships:

$$m_1-m_2=\left(\frac{\frac{1}{\lambda_1}-\frac{1}{\lambda_2}}{\frac{1}{\lambda_3}-\frac{1}{\lambda_4}}\right)(m_3-m_4)+12.5\left[\log\left(\frac{\lambda_1}{\lambda_2}\right)-\left(\frac{\frac{1}{\lambda_1}-\frac{1}{\lambda_2}}{\frac{1}{\lambda_3}-\frac{1}{\lambda_4}}\right)\cdot\log\left(\frac{\lambda_3}{\lambda_4}\right)\right].$$

The important feature of this equation is that it does not contain T. It is therefore a canonical equation of blackbody photometry which is the same for any four spectral measurements of a blackbody regardless of its temperature.

Suppose we now have a photoelectric chart deflection, d_y, at relative amplifier gain, G_y, expressed in magnitudes rather than decibels. Let the subscript refer to a particular radiation wavelength band, y for yellow and b for blue, and presume that the observations have been corrected for atmospheric extinction. Let there be a standard magnitude-color system (in practice we have used the Johnson BV system) called B and V. From the foregoing equation the following formulas must be valid:

$$V=(-2.5\log d_y+G_y)+A(2.5\log\frac{d_y}{d_b}-G_y+G_b)+C$$

and

$$B-V=D(2.5\log\frac{d_y}{d_b}-G_y+G_b)+E.$$

These equations are called the color equations or the transformation equations from the natural magnitude-color system of the telescope-photometer to the BV system. On a given night one obtains the observed parameters in the above equations for all objects measured. Among these are the standard stars for which V and $B-V$ are also known. The constant coefficients and additive constants A, C, D, and E in the color equations can therefore be determined by a least-square fit to the data. The transformation is then used to reduce the photometry to the BV system.

Of course a star is not exactly a blackbody because of its complicated opacity and radiative equilibrium, and there is a gradual variation with wave length of the moon's reflectivity. Furthermore, our photometry is rather broad band and not monochromatic. However, if response variations with the wavelength for V and y (and B and b) do not differ by more than the commercial tolerances for a filter and a photoemissive surface of the same type as was originally used to establish the BV system, these effects will produce errors much less than 1 percent. This is true even when the color corrections themselves are in a range of as high as 10–15 percent. A useful check on the photometry is the closeness of D to unity and of A to zero.

It should also be made clear that although the V magnitude can be defined in the following way:

$$V=-2.5\log\left[\frac{\int_0^\infty F_\lambda R_\lambda d\lambda}{\int_0^\infty R_\lambda d\lambda}\right]+\text{constant},$$

where F_λ is the stellar flux and R_λ is the spectral response of the V system, spectrophotometric control can be maintained indefinitely by the use of the color equations without ever knowing anything about R_λ. Indeed, the precision is superior to what would be obtained by ordinary laboratory techniques for measuring and correcting for R_λ using a nominal spectral shape for F_λ and evaluating integrals.

The photoelectric observations which calibrate the albedo map of the present investigation employed 10 BV standard stars measured before, during, and after the lunar photoelectric observations. Actually, a photoelectric ultraviolet color was also measured, the overall system being the Johnson-Morgan UBV system.

The ensuing calibration of the photography, according to the technique discussed in the text, implicitly assumes that in the connection between the spectral bands of photoelectric V and 649F + GG 14, there is no color term (that is, in the connection between the BV system and a photoelectric system for which the blue response is spectrometrically identical with B and the

yellow response is identical with 649F + GG 14, the coefficient A is zero). The color equation shows that this will not lead to error even if such an assumption is poorly founded, provided that the moon does not show a large dispersion in color index. This appears to be the case. Although Eastman Kodak emulsion 103a–D + 2.0 mm of Schott GG 11 filter has a spectral response almost identical with that of V, this spectroscopic emulsion is very grainy and is also too fast for a photometric exposure by our presently operational technique.

THE THEORY OF LAMBERT SCATTERING AND THE ABSOLUTE CALIBRATION OF NORMAL ALBEDO

Given a magnitude corresponding to full scale on a photoelectric trace from which points for the plate calibration are taken, the normal albedo to which it corresponds must be determined. This is done in two steps. First, determine the absolute specific intensity that would be exhibited by a Lambert scattering surface when placed at the distance from the sun corresponding to the time of the observation. Then, convert the V magnitude to an absolute specific intensity.

A Lambert surface is the ideal diffuse reflecting surface which absorbs no light and shines with a specific intensity constant over all directions. For the surface brightness thus defined to be consistent with the first law of thermodynamics, it must be proportional to the cosine of the angle of incidence (i) of the illuminator. For considerations of the normal albedo, the desired geometry requires that $\cos i=1$.

The specific intensity of a Lambert surface under solar illumination is derived as follows: Let the solar flux in the V band be F_V at the position in space occupied by the earth-moon system. Then the energy striking the Lambert surface in a unit area per unit time is F_V. Let the specific intensity in the V band exhibited by the surface be I_{VL}. In a given direction, θ (polar), ϕ (azimuth), with respect to the local normal, the total area perpendicular to this direction through which the beams passing in this direction will have come from the unit area is $\cos\theta$. Thus the radiant (V band) power per unit solid angle in this direction that comes from the unit area of Lambert surface is $I_{VL}\cos\theta$. The total V band power that is leaving the surface is obtained by integrating over the half space of solid angle above the surface. Equating this to the power arriving per unit area,

$$F_V=\int_0^{\pi/2}\int_0^{2\pi}(I_{VL}\cos\theta)\sin\theta\,d\theta\,d\phi.$$

Because the surface is lambertian, I_{VL} can be taken outside the integral and we obtain

$$I_{VL}=\frac{F_V}{\pi}\ \text{(power in the band per unit area per steradian)}.$$

Stebbins and Kron (1957) have measured the apparent V magnitude of the sun. Willstrop (1960) has measured the absolute value of F_λ (watts per A per cm^2) for 100 A bandwidths at various points in stellar spectra of stars of known V and B–V. This is sufficiently wide to effectively smooth the Fraunhofer lines and sufficiently narrow to be a reasonable mesh for a numerical integration over the V spectral response function. We can thus write

$$V=2.5\log F_V+\text{constant}$$

$$F_v=\frac{\int_0^\infty F_\lambda R_\lambda d\lambda}{\int_0^\infty R_\lambda d\lambda}.$$

Carrying out the integration in the second equation by using Willstrop's data and Johnson's (1955) tabulation of the V response function, one then solves for the constant in the first equation. F_V is thus evaluated.

The V magnitude corresponding to the lunar photoelectric observational scale of this study is also translatable into a flux using the foregoing two equations. The calibration of F_V thus provided is independent of color; however, the effective wavelength of the lunar F_V is somewhat longer than that of the sun because the moon is redder than the sun. Values have not been normalized to the same monochromatic wavelength, but normalization would lead to a small change at worst. There is also no a priori reason why a monochromatic evaluation will be more meaningful than one corresponding to a broad band. The F_V of a star is its radiative flux density at earth. In terms of the total radiative power the telescope receives from the star, F_V is merely this power divided by the area of the objective mirror, which is the area within which all the stellar photons count toward the energy transfer and outside of which none do (see fig. 9). Obviously the mirror has the necessary properties of being an area element that is perpendicular to the stellar direction and also one that is located at earth rather than somewhere closer to or farther from the star. The F_V of the moon can be changed to a specific intensity by dividing it by the solid angle of the celestial sphere imaged within the focal plane aperture. This is the correct solid angle because the area of

integration of specific intensity that is characteristic of the measurement, although it can be chosen anywhere along the light beam, will be common to both the stellar and the lunar measurement if it is chosen at the telescope entrance pupil (and, hence, is the circular area of the telescope objective mirror). If the area is thus chosen, the corresponding solid angle is that stated above, as can be seen in the object-image geometry (fig. 9). With the solid angle chosen as above, one accounts for (1) all the lunar light that is responsible for the photoelectric signal and (2) the entire stellar image and therefore the stellar flux—hence, the rationale for the above conversion to specific intensity.

With both the Lambertian and the observed lunar specific intensities evaluated as above, the normal albedo in the Johnson V band is evaluated according to definition by dividing the latter by the former.

U. S. GOVERNMENT PRINTING OFFICE : 1970 O - 373-263